

A 2.1 SOLAR MASS PULSAR MEASURED BY RELATIVISTIC ORBITAL DECAY

DAVID J. NICE AND ERIC M. SPLAVER
Physics Department, Princeton University
Princeton, NJ 08544

INGRID H. STAIRS
Department of Physics and Astronomy, University of British Columbia
6224 Agricultural Road, Vancouver, BC V6T 1Z1, Canada

OLIVER LÖHMER AND AXEL JESSNER
Max-Planck-Institut für Radioastronomie
Auf dem Hügel 69, D-53121 Bonn, Germany

MICHAEL KRAMER
University of Manchester, Jodrell Bank Observatory
Macclesfield, Cheshire, SK11 9DL, UK

AND

JAMES M. CORDES
Astronomy Department and NAIC, Cornell University
Ithaca, NY 14853

Submitted to the Astrophysical Journal, 15 June 2005; Revised, 31 July 2005

ABSTRACT

PSR J0751+1807 is a millisecond pulsar in a circular 6 hr binary system with a helium white dwarf secondary. Through high precision pulse timing measurements with the Arecibo and Effelsberg radio telescopes, we have detected the decay of its orbit due to emission of gravitational radiation. This is the first detection of the relativistic orbital decay of a low-mass, circular binary pulsar system. The measured rate of change in orbital period, corrected for acceleration biases, is $\dot{P}_b = (-6.4 \pm 0.9) \times 10^{-14}$. Interpreted in the context of general relativity, and combined with measurement of Shapiro delay, it implies a pulsar mass of $2.1 \pm 0.2 M_\odot$, the most massive pulsar measured. This adds to the emerging trend toward relatively high neutron star masses in neutron star–white dwarf binaries. Additionally, there is some evidence for an inverse correlation between pulsar mass and orbital period in these systems. We consider alternatives to the general relativistic analysis of the data, and we use the pulsar timing data to place limits on violations of the strong equivalence principle.

Subject headings: gravitation—binaries: general—pulsars: individual (PSR 0751+1807)

1. INTRODUCTION

A fundamental prediction of general relativity is the emission of gravitational radiation by binary systems. The consequent loss of energy and angular momentum from these systems causes their orbital periods to decrease (Peters 1964). Previous to the present work, relativistic orbit decay had been detected in five binary pulsar systems. Four of these systems consist of a mildly recycled pulsar bound to a second neutron star in an eccentric orbit (Taylor & Weisberg 1989; Stairs et al. 2002; Deich & Kulkarni 1996; Kramer et al. 2005). The fifth system, that of PSR J1141–6545, contains a young pulsar and a $\sim 1 M_\odot$ white dwarf in an eccentric orbit (Bailes et al. 2003).

In this paper, we report the measurement of the relativistic decay of PSR J0751+1807, a millisecond pulsar in a 6 hr orbit (Lundgren et al. 1995). This system differs in several ways from the other binaries in which relativistic decay has been detected. First, its rotation period of 3.4 ms is an order of magnitude smaller than the rotation periods of the pulsars in the other systems, implying greater accumulation of angular

momentum during its binary accretion phase. Second, its magnetic field is substantially lower than those of the other systems, presumably because of differences in orbital evolution and accretion (Bhattacharya 2002). Third, its orbit is extremely circular, with eccentricity under 2×10^{-6} , a consequence of tidal circularization during the late stages of the secondary (Phinney 1992). Fourth, the secondary to PSR J0751+1807 is a low mass helium white dwarf, several times lighter than the secondary stars in the other systems.

Measurements of relativistic orbital phenomena in binary systems yield constraints on the masses of the stellar components of the systems. Neutron star mass measurements, in turn, serve as probes of the properties of nuclear matter at high densities (e.g., Lattimer & Prakash 2001). The maximum achievable neutron star mass depends on the equation of state of nuclear matter. Soft equations of state, expected if the core of the neutron star is composed of non-nucleonic matter, predict the maximum neutron star mass $\lesssim 2 M_\odot$, while stiffer equations of state allow higher values.

Reviewing the field several years ago,

TABLE 1
SUMMARY OF OBSERVATIONS

Observatory	System	Dates	Frequency (MHz)	Bandwidth (MHz)	Number of TOAs	Typical Integration (min)	RMS Residual (μ s)
Arecibo	Mark III	1993.8–1994.4	430	8	1190	0.5	25
	Mark IV	1998.9–2004.1	430	10	1007	3.2	5
	Mark IV	1997.9–2001.5	1410	10	109	3.2	7
	WAPP	2004.1–2004.1	1145	50	562	0.5	10
	WAPP	2004.1–2004.1	1195	50	559	0.5	8
	WAPP	2004.1–2004.1	1395	50	559	0.5	8
	WAPP	2004.1–2004.1	1445	50	559	0.5	8
Effelsberg	EBPP	1997.0–2004.6	1409	56	490	7.0	7

Thorsett & Chakrabarty (1999) found all radio pulsar mass measurements to be consistent with a narrow underlying Gaussian mass distribution, $1.35 \pm 0.04 M_{\odot}$. More recent observations have found (1) neutron star masses in neutron star–neutron star binary systems lie in the range 1.18 to $1.44 M_{\odot}$; (2) PSR J1141–6454, a young pulsar in an eccentric orbit with a white dwarf secondary, has mass $1.30 M_{\odot}$; and (3) neutron stars in circular neutron star–wide dwarf systems may have somewhat larger masses, but the uncertainties are large (e.g., Nice et al. 2005).

Neutron star masses can also be measured in X-ray binary systems. Spectroscopic and eclipse observations typically yield neutron star mass measurements in the range 1.1 to $1.5 M_{\odot}$, but there is evidence for a few more massive neutron stars: $1.78 \pm 0.2 M_{\odot}$ for the neutron star in Cygnus X-2 (Orosz & Kuulkers 1999), $2.44 \pm 0.27 M_{\odot}$ for the neutron star in 4U1700–37 (Clark et al. 2002), and $2.27 \pm 0.17 M_{\odot}$ for the neutron star in Vela X-1 (Quaintrell et al. 2003). See the review papers by Lattimer & Prakash (2004) and Charles & Coe (2005) for further references.

We undertook high precision pulse timing observations of PSR J0751+1807 with the goal of measuring its orbital decay, both to test the expected relativistic behavior of its binary system and to deduce the pulsar and secondary star masses. In §2 we describe the observations in detail. In §3 we present results of fitting pulse timing models to the data. In §4 we use our measurements to place constraints on theories of relativistic gravity. In §5 we discuss the pulsar mass and the evolution of the binary system. In §6, we summarize the major points of the paper.

2. OBSERVATIONS

We observed PSR J0751+1807 for more than ten years using the 305 m telescope at Arecibo and the 100 m telescope at Effelsberg. The bulk of the Arecibo data were collected in campaigns of duration ~ 1 week over which all orbital phases were observed. Such campaigns were undertaken in November 1993, May 1999, May 2000, June/July 2001, May 2003, and January 2004. Additional data were collected at some other epochs in 1993–1994 and 1999–2000 (Figure 1). Effelsberg data were less concentrated, with observations spread evenly over several years and a single major campaign in February 2000. The two types of data complement

each other, with campaign data especially useful for measuring orbital elements, and with less concentrated observations important for determining pulse spin-down and astrometric parameters. Ultimately, all 5035 pulse arrival times from both observatories were combined and simultaneously fit to pulsar timing models (§3).

2.1. Arecibo Observations

Observations at Arecibo in 1993 and 1994 are described in Lundgren et al. (1995). The Princeton Mark III data acquisition system collected signals across a 8 MHz passband at 430 MHz using a 32-channel filter bank spectrometer with 100μ time constants. Observations from 1997 to 2004 employed the Princeton Mark IV coherent dedispersion system (Stairs et al. 2000). Most observations were made at 430 MHz with a 5 MHz passband, but some were made at 1410 MHz using a 10 MHz passband. Observations typically lasted 29 minutes and were analyzed in blocks of 190 s.

The January 2004 Arecibo campaign included extensive observations at radio frequencies 1120 to 1470 MHz. These data were collected with four

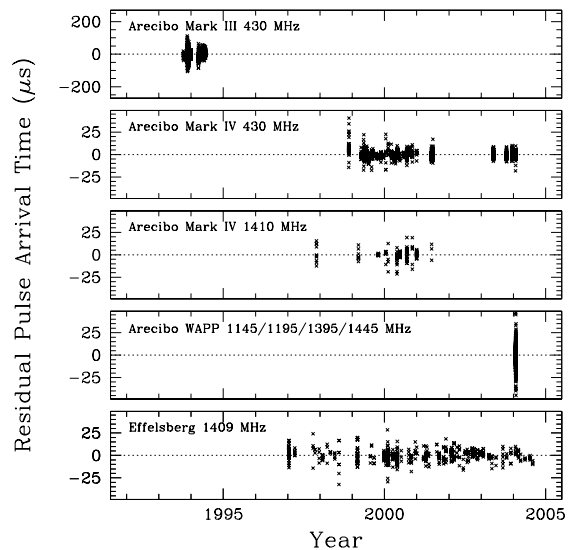


FIG. 1.— Residual pulse arrival times after removing the best fitting pulse timing model. Points are segregated by observatory, frequency, and data acquisition system. Note the difference in vertical scales.

TABLE 2
TIMING MODEL PARAMETERS^a

Basic Timing Model (Three Post-Keplerian Parameters)	
Ecliptic longitude, λ	116°33362028(2)
Ecliptic latitude, β	-2°807548(2)
Proper motion in λ , $\mu_\lambda = \cos \beta (d\lambda/dt)$ (mas/yr)	-0.35(3)
Proper motion in β , μ_β (mas/yr)	-6(2)
Parallax (mas), π	1.6(8)
Rotation frequency, ν_0 (s ⁻¹)	287.457858630106(2)
Rotation frequency derivative, ν_1 (s ⁻²) ^b	-6.4337(4) $\times 10^{-16}$
Epoch, t_0 (MJD [TDB])	51800.0
Dispersion measure, DM_0 (pc cm ⁻³) ^c	30.2489(3)
Dispersion measure derivative, DM_1 (pc cm ⁻³ yr ⁻¹) ...	-0.00017(1)
Orbital period, P_b (days) ^b	0.263144266723(5)
Projected semi-major axis, x (lt-s)	0.3966127(6)
Eccentricity, e	5(11) $\times 10^{-7}$
Time of ascending node, t_{asc} (MJD [TDB])	51800.21573411(2)
Orbital period derivative, \dot{P}_b (unitless)	-6.2(8) $\times 10^{-14}$
Shapiro parameters, r and s	see Figure 2
General Relativistic Timing Model (Two Post-Keplerian Parameters)	
Cosine of inclination angle, $\cos i$	0.41 ^{+0.11} _{-0.07}
Pulsar mass, m_1 (M _⊙)	2.1(2)
Secondary mass, m_2 (M _⊙)	0.191(15)

^aFigures in parentheses are 68% confidence uncertainties in the last digit quoted.

^bObserved value, not corrected for acceleration biases; see Table 3.

^cFormal uncertainty in the timing fit. No attempts were made to correct for pulse shape evolution over frequency.

Wideband Arecibo Pulsar Processors (WAPPs). Each WAPP calculated autocorrelations of 192 lags across a 50 MHz passband in each sense of polarization. Autocorrelations were accumulated for 32 μ s and then summed into folded pulse profiles with 256 bins across the pulse period. The four WAPP passbands were centered at 1145, 1195, 1395, and 1445 MHz. Data from each of the four passbands were reduced independently.

Each data acquisition system folded the signals modulo the pulse period using a precomputed ephemeris. A pulse time of arrival (TOA) was calculated from each data block by fitting a high quality template profile to the data profile and adding the phase offsets thus measured to the observation start times. A suitable number of pulse periods was added to the TOA to make it fall near the center of the observation. Start times were referenced to the observatory time standard and later corrected to UTC and, ultimately, TT(BIPM03).

2.2. Effelsberg Observations

At Effelsberg, timing data of PSR J0751+1807 have been collected since 1997, with observations made approximately once a month using a 1300–1700 MHz tunable HEMT receiver at a center frequency of 1409 MHz. All observations employed the Effelsberg–Berkeley Pulsar Processor (EBPP) as the data acquisition system, correcting the dispersion smearing of the signal using coherent dedispersion (Backer et al. 1997).

In total power mode, the EBPP provided 32 channels across a total of 56 MHz for each sense of circular polarization. The output signals of each channel were fed into digital dedisperser boards for coherent on-line dedispersion and were synchronously folded at the pulse

period over 7 min integration times. The signal-to-noise ratio varied between 3 and 10 for the individual integrations, depending on interstellar scintillation. As with the Arecibo data, TOAs were calculated by fitting the data to high quality template profiles and calculating the phase offset relative to the observation start times. Start times were referenced to the observatory hydrogen maser clock, corrected to UTC(NIST) using the signals from the Global Positioning System (GPS), and finally corrected to TT(BIPM03).

3. TIMING ANALYSIS

3.1. Basic Timing Model (Three Post-Keplerian Parameters)

The TOA measurements were fit to pulse timing models using the TEMPO software package¹. The basic timing model had 23 parameters and 5012 degrees of freedom. The results of the fit is summarized in Table 2, and residual arrival times after removing the timing model are plotted in Figure 1. Pulsar rotation was parameterized by spin frequency, ν_0 , and its derivative, ν_1 . Earth motion was modeled by the JPL DE405 Ephemeris (Standish 1998). To minimize covariances between components of position and proper motion, astrometric results are presented in ecliptic coordinates, calculated by rotating the coordinates of the solar system ephemeris about the x axis by the obliquity of the Earth, $\epsilon_0 = 84381''412$. Arbitrary time offsets were fit between data sets collected at different observatories, at different frequencies, or with different equipment. Interstellar dispersion was modeled with a dispersion measure, DM, changing linearly with time, $DM(t) = DM_0 + DM_1 t$,

¹ <http://pulsar.princeton.edu/tempo>

while dispersion within the solar system was calculated using an analytical model of the solar wind (§3.5).

Orbital motion was calculated using the “ELL1” relativistic orbital model (Appendix A of Lange et al. 2001). A combination of five Keplerian and three post-Keplerian orbital elements were fit to the data. The Keplerian orbital elements were the orbital period, P_b ; the semi-major axis projected into the line of sight, $x = (a_1 \sin i)/c$, where i is the inclination and c is the speed of light; the time of passage through the ascending node, t_{asc} ; and two Laplace-Lagrange parameters, η and κ , which parameterize the eccentricity. Since neither of these were statistically significant, we report total eccentricity, $e = (\eta^2 + \kappa^2)^{1/2}$; the value in Table 2 should be taken as an upper limit.

The three post-Keplerian parameters were the time rate of change of orbital period, \dot{P}_b , and the shape and range parameters of Shapiro delay, s and r . The latter are defined by the perturbation in arrival time, Δt , imposed by Shapiro delay; for a nearly circular orbit, this is

$$\Delta t = -2r \ln\{1 - s \sin[(2\pi/P_b)(t - t_{\text{asc}})]\}, \quad (1)$$

where t is the pulse arrival time.

The best fit parameters are given in Table 2 under the heading “Basic Timing Model.” The most important new measurement is the relativistic period decay rate,

$$\dot{P}_b = -(6.2 \pm 0.8) \times 10^{-14}, \quad (2)$$

discussed further below. The two Shapiro parameters, r and s , are highly covariant, and the confidence regions are non-elliptical. The values allowed by the timing data are shown in Figure 2.

3.2. The Basic Timing Model under General Relativity

The basic timing model provides an excellent fit to the data without reference to a specific theory of gravitation. The implications of this for gravitation

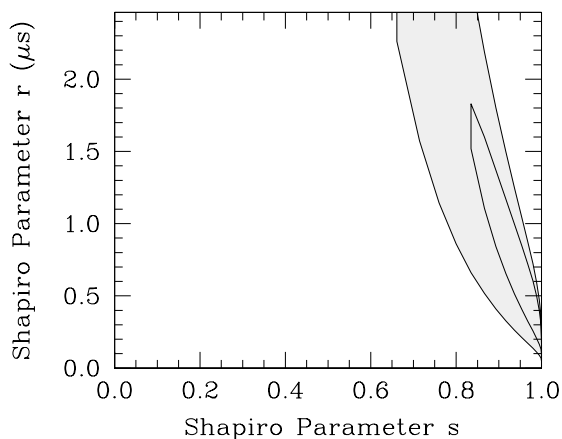


FIG. 2.— Constraints on Shapiro delay parameters r and s from the basic timing analysis. Inner and outer contours delimit 68% and 95% confidence regions.

theory are discussed below (§4). Here, these results are interpreted in terms of general relativity.

Under general relativity, the post-Keplerian parameters are related to the masses of the pulsar, m_1 , and the secondary star, m_2 , and the inclination of the orbit:

$$\begin{aligned} (\dot{P}_b)_{\text{GR}} = & - \left(\frac{192\pi}{5}\right) \left(\frac{2\pi}{P_b}\right)^{5/3} \left(1 + \frac{73}{24}e^2 + \frac{37}{96}e^4\right) \\ & \times \frac{1}{(1-e^2)^{7/2}} T_{\odot}^{5/3} \frac{m_1 m_2}{(m_1 + m_2)^{1/3}}, \quad (3) \end{aligned}$$

$$r = T_{\odot} m_2, \quad (4)$$

and

$$s = \sin i, \quad (5)$$

where masses are in solar units and $T_{\odot} = GM_{\odot}/c^3 = 4.925490947 \times 10^{-6}$ s. The masses and inclination are related by the Keplerian mass function,

$$f_1 \equiv \frac{(m_2 \sin i)^3}{(m_1 + m_2)^2} = \frac{x^3}{T_{\odot}} \left(\frac{2\pi}{P_b}\right)^2. \quad (6)$$

Under general relativity, the measured values of orbital decay and Shapiro delay yield the constraints on m_1 , m_2 , and i shown in Figure 3a. Evidently, meaningful constraints on the individual masses can be attained only by combining the Shapiro delay and orbit decay measurements. Given this circumstance, it is useful to directly incorporate general relativity into the timing analysis and to explicitly consider m_1 and m_2 as independent variables.

3.3. General Relativistic Timing Model (Two Post-Keplerian Parameters); Stellar Masses

We undertook a series of timing analyses in which general relativity was assumed to hold, so that there were only two independent post-Keplerian parameters instead of the three parameters of the basic timing model. This timing model had a total of 22 parameters and 5013 degrees of freedom. We chose the independent variables to be $\cos i$ and m_2 . We analyzed a uniform grid of values of these quantities, restricting $\cos i$ to be between 0 and 1, and m_2 to be between 0 and $0.5 M_{\odot}$. For each value of $\cos i$ and m_2 , the values of \dot{P}_b , m_1 , r , and s were calculated using equations 3 through 6. The TOAs were fit to a timing solution with these parameters held fixed but all other parameters allowed to vary. For each combination of $\cos i$ and m_2 , the statistic $\Delta\chi^2 = \chi^2 - \chi_{\text{min}}^2$, of the best fit timing solution was recorded, where χ^2 is the goodness-of-fit of a particular timing solution and χ_{min}^2 is the global minimum from all grid points. Fits with acceptable values of $\Delta\chi^2$ at the 68% and 95% confidence levels are shown in Figures 3b and 4.

The values of $\cos i$, m_1 , and m_2 and their uncertainties, were calculated following the procedure outlined in Appendix A of Splaver et al. (2002). Essentially this was a Bayesian analysis with uniform priors in $\cos i$ and m_2 . A probability was assigned to each grid point based on its $\Delta\chi^2$. After suitable normalization, the probabilities of all points associated with a given range of $\cos i$ (or m_1 or m_2) were summed to calculate a probability distribution

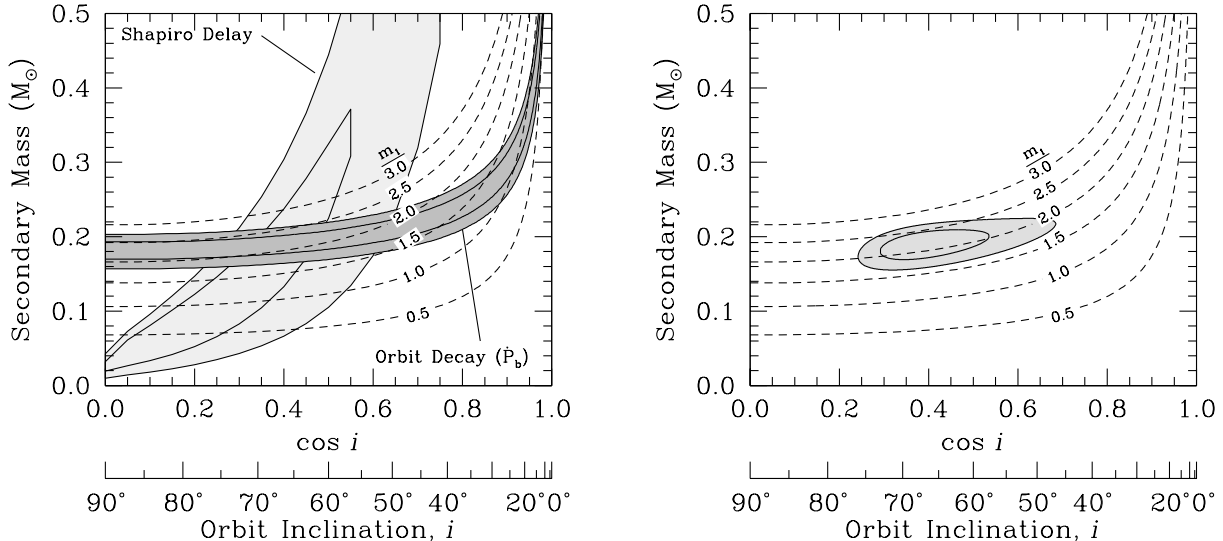


FIG. 3.— Constraints on $\cos i$ and m_2 . Dashed lines indicate values of m_1 according to equation 6. (a) *Left plot*: Constraints from the basic timing model, with three post-Keplerian parameters (orbital decay and two Shapiro delay parameters), cast into inclination and mass values via equations 3 through 6. (b) *Right plot*: Constraints from the general relativistic timing model, with two post-Keplerian parameters (inclination and secondary mass). In each plot, inner and outer contours correspond to 68% and 95% confidence limits.

function. The confidence intervals derived from these probability distributions were:

$$\cos i = \begin{cases} 0.41^{+0.11}_{-0.07} & (68\% \text{ confidence}) \\ 0.41^{+0.27}_{-0.13} & (95\% \text{ confidence}), \end{cases} \quad (7)$$

$$m_1 = \begin{cases} 2.1 \pm 0.2 M_\odot & (68\% \text{ confidence}) \\ 2.1^{+0.4}_{-0.5} M_\odot & (95\% \text{ confidence}), \end{cases} \quad (8)$$

and

$$m_2 = \begin{cases} 0.191 \pm 0.015 M_\odot & (68\% \text{ confidence}) \\ 0.191^{+0.033}_{-0.029} M_\odot & (95\% \text{ confidence}). \end{cases} \quad (9)$$

3.4. Lower Limit on Pulsar Mass from \dot{P}_b Alone

While there is no reason to doubt the detection of Shapiro delay, it is worth noting that the orbit decay measurement alone provides some evidence for a very massive neutron star. We calculated a probability distribution function for m_1 assuming a uniform *a priori* distribution for $\cos i$, appropriate for randomly oriented orbits, and assuming \dot{P}_b is drawn from the Gaussian distribution implied by its measurement uncertainty. The distribution of m_1 calculated under these assumptions gives lower limits $m_1 > 1.75 M_\odot$ (68% confidence) and $m_1 > 0.88 M_\odot$ (95% confidence).

3.5. Solar Wind

Radio signals are dispersed by electrons in the interstellar medium and in the solar wind. Because the solar wind is variable and unpredictable, its contribution can degrade the accuracy of pulsar timing models. The problem is particularly acute for PSR J0751+1807 because of its low ecliptic latitude. Dispersion by the solar wind imposed delays of up to $\sim 12 \mu\text{s}$ in the TOAs in our data set. We excluded all observations for which the line of sight to the pulsar passed within 15° of the

sun. We found that changing this cutoff to 30° or to 0° had little impact on our results.

In principle, observations at multiple radio frequencies at every epoch would allow the dispersion to be measured and removed; in practice, it is difficult to measure high precision TOAs at two or more widely spaced frequencies, so it becomes necessary to use an analytic model of the solar wind and average the results over many epochs. We modeled the electron density in the solar wind as $n_e(r) = n_0(1\text{AU}/r)^2$, where r is the distance to the

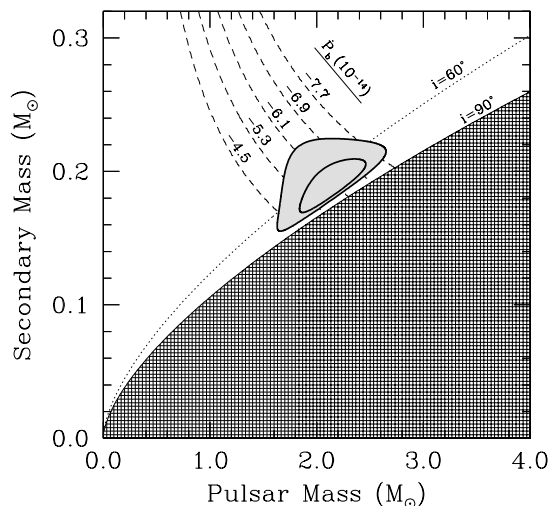


FIG. 4.— Constraints on pulsar and secondary masses from the general relativistic timing model. Confidence limits of 68% and 95% are shown. These are the same constraints as the right plot of figure 3, cast into a different parameterization. The shaded region in the lower left is disallowed by the Keplerian mass function. Dashed lines show constraints from \dot{P}_b alone. A dotted line indicates inclination $i = 60^\circ$.

sun and n_0 is the electron density at 1 AU. We found the best fits to the data had $n_0 = 9.6 \pm 3.0 \text{ pc cm}^{-3}$. Within this uncertainty range, the particular value of n_0 used had little impact in the rotation and binary parameters derived in the timing fit; we used a fixed value of $n_0 = 9.6 \text{ cm}^{-3}$ to calculate the rotation and binary parameters in Table 2.

The pulsar’s astrometric parameters—position, proper motion, and parallax—exhibit high covariances with n_0 and with time changes in n_0 . To estimate values and uncertainties for these parameters, we fit a grid of timing solutions with n_0 between 6.6 and 12.6 pc cm^{-3} , and with the time derivative of n_0 between -1.5 and $+1.5 \text{ pc cm}^{-3} \text{ yr}^{-1}$. We use the extreme values from these timing fits to calculate the uncertainties on position, proper motion, and parallax given in Table 2.

Observations of another pulsar, J1713+0747, over a similar period of time found a marginally smaller solar wind electron density, $n_0 = 5 \pm 4 \text{ pc cm}^{-3}$ (Splaver et al. 2005). Despite differing by a factor of two, the n_0 values from the two pulsars are in statistical agreement.

4. PROBING STRONG FIELD GRAVITY

Pulsars are well established testbeds for relativity. Observations of the neutron star–neutron star binary PSR B1913+16 have established that its orbit decays at the rate predicted by general relativity within 0.3% (Taylor & Weisberg 1989; Weisberg & Taylor 2003). However, this test of relativity is of limited use for constraining violations of the strong equivalence principle (SEP) because of the similar self-energies of the two neutron stars. More useful for probing this aspect of gravitation are neutron star–white dwarf binaries, in which the radically different self-energies of the two stars would generate excess gravitational wave energy loss under SEP-violating theories. A succinct review is given by Arzoumanian (2003) (see also Stairs 2003; Will & Zaglauer 1989; Goldman 1992; Lange et al. 2001; Gérard & Wiaux 2002).

The observed change in the orbital period of PSR J0751+1807 is $(\dot{P}_b/P_b)_{\text{obs}} = (-2.7 \pm 0.4) \times 10^{-18} \text{ s}^{-1}$. We consider five possible mechanisms for generating changes in the orbital period: acceleration of the binary system relative to the Earth; changes in the gravitational constant, i.e., nonzero \dot{G} ; changes in the masses of the component stars; energy loss from the binary due to quadrupole gravitational radiation, as in general relativity; and energy loss due to dipole radiation, as in SEP-violating theories. Contributions from tidal interactions between the two stars are likely not to be important (e.g., Smarr & Blandford 1976). The observed decay rate is the sum of the five contributions:

$$\left(\frac{\dot{P}_b}{P_b}\right)_{\text{obs}} = \left(\frac{\dot{P}_b}{P_b}\right)_A + \left(\frac{\dot{P}_b}{P_b}\right)_{\dot{G}} + \left(\frac{\dot{P}_b}{P_b}\right)_{\dot{m}} + \left(\frac{\dot{P}_b}{P_b}\right)_Q + \left(\frac{\dot{P}_b}{P_b}\right)_D. \quad (10)$$

We address each of these terms in turn.

The first term, acceleration biases, arises from the proper motion of the pulsar, acceleration toward the Galactic plane (z -acceleration), and Galactic rotation (see Damour & Taylor 1991, for details). The biases for

TABLE 3
BIASES OF PULSAR AND ORBITAL PERIOD DERIVATIVES

Quantity	\dot{P}	\dot{P}_b
<i>Measurement . . .</i>		
Uncertainty	7.7860×10^{-21}	-6.2×10^{-14}
	$\pm 0.0005 \times 10^{-21}$	$\pm 0.8 \times 10^{-14}$
<i>Acceleration biases . . .</i>		
Proper motion	0.35×10^{-21}	0.2×10^{-14}
z -acceleration	-0.19×10^{-21}	-0.1×10^{-14}
Galactic rotation	0.19×10^{-21}	0.1×10^{-14}
<i>Intrinsic value . . .</i>		
Measurement–Bias	7.44×10^{-21}	-6.4×10^{-14}
Uncertainty	$\pm 0.4 \times 10^{-21}$	$\pm 0.9 \times 10^{-14}$

PSR J0751+1807 are listed in Table 3. These values were calculated using the measured proper motion of 6 mas yr^{-1} , and using a distance of 1.15 kpc, derived from the dispersion measure of the pulsar using the NE2001 galactic electron density model (Cordes & Lazio 2002). To be conservative, we assign an uncertainty equal to the total bias (i.e., 100% uncertainty). The bias of \dot{P}_b is much smaller than its measurement uncertainty and essentially negligible.²

The second term in Equation 10, due to \dot{G} , can be shown negligible by appeal to other binary pulsars. The change in orbital period due to nonzero \dot{G} is approximately $(\dot{P}_b/P_b)_{\dot{G}} \simeq -2(\dot{G}/G)$. This expression neglects the effects of \dot{G} on the energy content of the stars themselves; a more precise expression is given in Nordtvedt (1990), but is not necessary for the purposes of the present paper. Because the same expression for $(\dot{P}_b/P_b)_{\dot{G}}$ holds for *any* binary pulsar system, the binary with the lowest value of this expression sets an upper limit on it for *all* pulsars. The best limit comes from PSR J1713+0737, for which $\dot{P}_b/P_b \leq 1 \times 10^{-19} \text{ s}^{-1}$ (Splaver et al. 2005), more than an order of magnitude smaller than our value for PSR J0751+1807. A comparable limit on $(\dot{P}_b/P_b)_{\dot{G}}$ can be set using limits on \dot{G} from lunar laser ranging measurements, which have found $\dot{G}/G = (1.3 \pm 2.9) \times 10^{-20} \text{ s}^{-1}$ (Williams et al. 2004). In any case, \dot{G} effects are unimportant for PSR J0751+1807.

The third term arises if one of the component stars is losing mass (Esposito & Harrison 1975; Lavagetto et al. 2005). First, we consider mass loss from the pulsar. The pulsar’s measured spin down rate implies that it is losing energy at a rate $\dot{E} = 4\pi^2\nu_0\nu_1 I_1$, where I_1 is the moment of inertia of the pulsar. Assuming the pulsar outflow is relativistic, this energy loss rate is equivalent to a mass loss rate of $\dot{m}_1 = \dot{E}/c^2 = 4\pi^2\nu_0\nu_1 I_1/c^2 = -4 \times 10^{-21} \text{ M}_\odot \text{ s}^{-1} (I_1/10^{45} \text{ g cm})$. The resulting change in the orbital period is $(\dot{P}_b/P_b)_{\dot{m}} = -2\dot{m}_1(m_1 + m_2)^{-1} \simeq -4 \times 10^{-21} \text{ s}^{-1}$, depending on the precise values of m_1 , m_2 , and I_1 . This is three orders of magnitude smaller than the measured value and, so mass loss can be

² The same phenomena shift the pulse period derivative, $\dot{P} = \nu_1/\nu_0^2$, a few percent away from its intrinsic value, but this is of no practical consequence.

neglected.

Next, we consider mass loss from the white dwarf companion. I. Wasserman (private communication) has pointed out that mass flow from the white dwarf could arise from irradiation of the white dwarf by the pulsar. If such an outflow were directed predominantly opposite the motion of the white dwarf, it would induce a negative \dot{P}_b . Given the geometry of the PSR J0751+1807 system, a white dwarf of low mass might capture sufficient the pulsar flux to produce such an outflow, although there is no reason to expect the flow to be collimated tangential to the orbit. The presence of an ionized outflow would give rise to variations in the dispersion measure of the pulsar over the course of its orbit and, depending on the orbital geometry, might even cause eclipses. However, PSR J0751+1807 exhibits neither eclipses nor orbital variability in its dispersion measure. To search for the latter, we analyzed multi-frequency observations made in January 2004 by dividing the orbit into ten equal length sections and separately measuring the dispersion measure in each section. We found no significant variation in dispersion measure over the course of the orbit, with a conservative upper bound of $\Delta\text{DM} < 4 \times 10^{-4} \text{ pc cm}^{-3} = 1 \times 10^{15} \text{ cm}^{-2}$. This is strong, but not definitive, evidence against an outflow; it is possible to imagine scenarios with small orbital inclinations in which the pulsar irradiation directs the outflow away from our line of sight. Optical observations of the companion find it to be relatively cool, further evidence that a significant wind is unlikely (van Kerkwijk et al. 2005; M. van Kerkwijk, private communication).

The expressions for $(\dot{P}_b/P_b)_Q$ and $(\dot{P}_b/P_b)_D$ in Equation 10 depend on gravitational theory. In general relativity, $(\dot{P}_b/P_b)_Q$ is given by Equation 3, while $(\dot{P}_b/P_b)_D = 0$. In some SEP-violating theories, the quadrupole term equals the general relativistic expression, while the dipole contribution has the form

$$\left(\frac{\dot{P}_b}{P_b}\right)_D = -\left(\frac{2\pi}{P_b}\right)^2 T_\odot \left(\frac{G_*}{G}\right) \frac{m_1 m_2}{m_1 + m_2} (\alpha_{c1} - \alpha_{c2})^2. \quad (11)$$

where α_{c1} and α_{c2} are the couplings of the pulsar and the secondary star, respectively, to the scalar field, and G_* is the “bare” gravitational constant.

To measure or constrain the dipole term $(\dot{P}_b/P_b)_D$ using Equation 10, it is necessary to know the quadrupole term $(\dot{P}_b/P_b)_Q$, which in turn requires knowing m_1 and m_2 by means other than the measured \dot{P}_b . For PSR J0751+1807, there are no independent high precision measurements of m_1 and m_2 , so we must consider all combinations of m_1 and m_2 which fall within the Shapiro delay 95% confidence contour (Fig 3a) and have reasonable neutron star masses, $1 M_\odot < m_1 < 3 M_\odot$ (Lattimer & Prakash 2004). For these masses, the predicted general relativistic values of $(\dot{P}_b/P_b)_Q$ range from $-1.1 \times 10^{-18} \text{ s}^{-1}$ to $-1.4 \times 10^{-17} \text{ s}^{-1}$. The largest negative allowed value of $(\dot{P}_b/P_b)_D = (\dot{P}_b/P_b)_{\text{obs}} - (\dot{P}_b/P_b)_Q$, is $-4.1 \times 10^{-18} \text{ s}^{-1}$ (95% confidence). This arises at the smallest values of m_1 and m_2 that fall within the constraints, and corresponds to a difference in coupling strengths

$$(\alpha_{c1} - \alpha_{c2})^2 < 7 \times 10^{-5}. \quad (12)$$

This improves by a factor of a few on previously published upper limits from PSRs B0655+64 and J1012+5307 (Arzoumanian 2003; Lange et al. 2001). A result comparable to it can be derived from the measurements of the PSR J1141–6545 orbit presented in Bailes et al. (2003). In fact, in generalized tensor-scalar theories of gravity, the latter pulsar is likely to be the most constraining among known pulsar–white dwarf binaries. Its eccentric orbit gives rise to several relativistic phenomena, allowing its stellar masses to be measured independently of \dot{P}_b (Esposito-Farese 2004).

In Brans-Dicke theory, the coupling to star i is $\alpha_{ci} = 2s_i(2 + \omega_{\text{BD}})^{-1}$, where $s_i = -\partial \ln m_i / \partial \ln G$, the “sensitivity” of star i , is the change in its binding energy as a function of G , and where ω_{BD} is the Brans-Dicke coupling constant. Estimates of s_1 range from 0.1 to 0.3, depending on the neutron star equation of state (Will & Zaglauer 1989). The sensitivity of the white dwarf is negligible. The limit on coupling strengths (Eqn. 12) places a lower limit $\omega_{\text{BD}} > 1300(s_1/0.2)^2$ on the Brans-Dicke coupling constant. This limit is higher than previous constraints from pulsar work, but lower than the best limit attained by other means, $\omega_{\text{BD}} > 40000$, from radio ranging to the Cassini probe (Bertotti et al. 2003).

5. DISCUSSION

The mass of PSR J0751+1807 is the largest measured for any pulsar. As shown in Figure 5, pulsars in circular orbits with helium white dwarf companions tend to have masses greater than the canonical value of $1.35 M_\odot$. This is in contrast to pulsars and secondary stars in neutron star–neutron binaries, which fall within the range $1.18\text{--}1.44 M_\odot$ (§1). The relatively high masses of pulsars in neutron star–white dwarf systems presumably result from extended mass accretion during the late stages of their evolution.

An inverse correlation between orbital period and pulsar mass is apparent in Figure 5. Any such relation is likely to be complicated by the different evolutionary paths followed by different systems. The four systems with the longest orbital periods, those of PSRs J1713+0747, B1855+09, J0437–4715, and J1909–3744, are classical wide millisecond pulsar–helium white dwarf binaries, which underwent extended stable

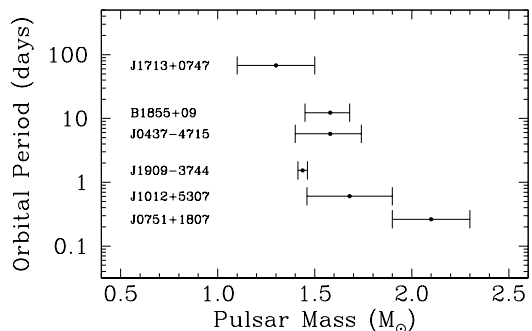


FIG. 5.— Measured pulsar masses in circular pulsar–helium white dwarf binary systems as a function of orbital period. Data are from this paper, Jacoby et al. (2005), Lange et al. (2001), van Straten et al. (2001), and Nice et al. (2005), and references therein.

mass transfer. In the library of evolutionary tracks calculated by Podsiadlowski et al. (2002), such systems show an inverse correlation between orbital period and pulsar mass, although there is a wide spread in pulsar mass for a given orbital period. In these calculations, it was assumed that half of the mass lost by the secondary was accreted onto the neutron star; whether the mass accreted onto the neutron star is, in fact, proportional to the mass lost by the secondary remains an open question.

PSRs J0751+1807 and J1012+5307, with their short orbital periods, provide a challenge to binary evolution theories. Evolution calculations tend not to produce systems with binary periods close to the orbital period of PSR J0751+1807 at the end of mass transfer. Its orbital period falls above the periods of ultracompact systems but below the periods of standard pulsar–white dwarf binaries (e.g., Podsiadlowski et al. 2002). Ergma et al. (2001) are able to produce the properties of the PSR J0751+1807 system by invoking magnetic braking and heating of the secondary by irradiation from the pulsar. The latter effect drives mass loss in the secondary, increasing the orbital separation and preventing the binary from shrinking into an ultracompact system. This picture is supported by optical observations, which find that the secondary lacks a hydrogen envelope and that it has cooled rapidly (van Kerkwijk et al. 2005).

6. SUMMARY

The orbit of PSR J0751+1807 decays at a rate of $\dot{P}_b = -(6.4 \pm 0.9) \times 10^{-14}$. This is in line with the expected value from general relativity. Combined with Shapiro delay measurements, it implies the pulsar and secondary star masses are $2.1 \pm 0.2 M_\odot$ and $0.191 \pm 0.15 M_\odot$, respectively. The mass of PSR J0751+1807 is the largest recorded for a pulsar, and it may imply greater mass

is transferred in tighter low mass neutron star binary systems than in wider systems.

The maximum mass attainable by a neutron star depends on the stars composition and the equation of state of nuclear matter. Lattimer & Prakash (2001) calculated neutron star mass–radius relationships for a number of plausible equations of state. They found that models with exotic components, such as pure quark stars or mixed phases with kaon condensate or strange quark matter, allow neutron stars to attain masses no higher than $\sim 2 M_\odot$. While the measurement of the PSR J0751+1807 mass is nominally above this limit, the measurement uncertainty is not yet small enough to draw firm conclusions on this point.

The uncertainty in the measurement of \dot{P}_b scales with observation span to the -2.5 power for uniformly sampled data. The precision of this measurement can, therefore, be increased dramatically with a relatively small number of observations over the next few years. The Shapiro delay measurement, because it has no such time dependence, will improve more slowly, and hence uncertainty in the Shapiro delay (and hence in the inclination) will ultimately dominate the uncertainty in the mass measurement.

We thank I. Wasserman for useful discussions. We thank D. Backer, A. Lommen, and K. Xilouris for collaborating in the collection of portions of the Arecibo data. The Arecibo Observatory is a facility of the National Astronomy and Ionosphere Center, operated by Cornell University under a cooperative agreement with the National Science Foundation. DJN and JMC are supported by NSF grants AST-0206205 (to Princeton), and AST-0206036 (to Cornell), respectively. IHS holds an NSERC UFA and is supported by a Discovery Grant.

REFERENCES

- Arzoumanian, Z. 2003, in *Radio Pulsars*, ed. M. Bailes, D. J. Nice, & S. Thorsett (San Francisco: Astronomical Society of the Pacific), 69
- Backer, D. C., Dexter, M. R., Zepka, A., D., N., Wertheimer, D. J., Ray, P. S., & Foster, R. S. 1997, *PASP*, 109, 61
- Bailes, M., Nice, D. J., & Thorsett, S., eds. 2003, *Radio Pulsars* (San Francisco: Astronomical Society of the Pacific)
- Bailes, M., Ord, S. M., Knight, H. S., & Hotan, A. W. 2003, *ApJ*, 595, L49
- Bertotti, B., Iess, L., & Tortora, P. 2003, *Nature*, 425, 374
- Bhattacharya, D. 2002, 23, 67
- Charles, P. A. & Coe, M. J. 2005, in *Compact Stellar X-ray Sources*, ed. W. H. G. Lewin & M. van der Klis (Cambridge University Press), in press, astro-ph/0308020
- Clark, J. S., Goodwin, S. P., Crowther, P. A., Kaper, L., Fairbairn, M., Langer, N., & Brocksopp, C. 2002, *A&A*, 392, 909
- Cordes, J. M. & Lazio, T. J. W. 2002, astro-ph/0207156
- Damour, T. & Taylor, J. H. 1991, *ApJ*, 366, 501
- Deich, W. T. S. & Kulkarni, S. R. 1996, in *Compact Stars in Binaries: IAU Symposium 165*, ed. J. van Paradijs, E. P. J. van del Heuvel, & E. Kuulkers (Dordrecht: Kluwer), 279
- Ergma, E., Sarna, M. J., & Gerskevits-Antipova, J. 2001, *MNRAS*, 321, 71
- Esposito, L. W. & Harrison, E. R. 1975, *ApJ*, 196, L1
- Esposito-Farese, G. 2004, contribution to 10th Marcel Grossmann meeting, gr-qc/0402007
- Gérard, J.-M. & Wiaux, Y. 2002, *Phys. Rev. D*, 66, 1
- Goldman, I. 1992, *ApJ*, 390, 494
- Jacoby, B. A., Hotan, A., Bailes, M., Ord, S., & Kulkarni, S. R. 2005, *ApJ*, in press, astro-ph/0507420
- Kramer, M., Lorimer, D. R., Lyne, A. G., McLaughlin, M., Burgay, M., D’Amico, N., Possenti, A., Camilo, F., Freire, P. C. C., Joshi, B. C., Manchester, R. N., Reynolds, J., Sarkissian, J., Stairs, I. H., & Ferdman, R. D. 2005, in *Proc. of the 22nd Texas Symposium on Relativistic Astrophysics*, in press, astro-ph/0503386
- Lange, C., Camilo, F., Wex, N., Kramer, M., Backer, D., Lyne, A., & Doroshenko, O. 2001, *MNRAS*, 326, 274
- Lattimer, J. H. & Prakash, M. 2004, *Science*, 304, 536
- Lattimer, J. M. & Prakash, M. 2001, *ApJ*, 550, 426
- Lavagetto, G., Burderi, L., D’Antona, F., Di Salvo, T., Iaraia, R., & Robba, N. R. 2005, *MNRAS*, in press, astro-ph/0502422
- Lundgren, S. C., Zepka, A. F., & Cordes, J. M. 1995, *ApJ*, 453, 419
- Nice, D. J., Splaver, E. M., & Stairs, I. H. 2005, in *Binary Radio Pulsars*, ed. F. A. Rasio & I. H. Stairs (San Francisco: Astronomical Society of the Pacific), in press
- Nordtvedt, K. 1990, *Phys. Rev. Lett.*, 65, 953
- Orosz, J. A. & Kuulkers, E. 1999, *MNRAS*, 305, 132
- Peters, P. C. 1964, *Phys. Rev.*, 136, 1224
- Phinney, E. S. 1992, *Philos. Trans. Roy. Soc. London A*, 341, 39
- Podsiadlowski, P., Rappaport, S., & Pfahl, E. D. 2002, *ApJ*, 565, 1107
- Quaintrell, H., Norton, A. J., Ash, T. D. C., Roche, P., Willems, B., Bedding, T. R., Baldry, I. K., & Fender, R. P. 2003, *A&A*, 313, 313
- Rasio, F. A. & Stairs, I. H., eds. 2005, *Binary Radio Pulsars* (San Francisco: Astronomical Society of the Pacific), in press
- Smarr, L. L. & Blandford, R. 1976, *ApJ*, 207, 574
- Splaver, E. M., Nice, D. J., Arzoumanian, Z., Camilo, F., Lyne, A. G., & Stairs, I. H. 2002, *ApJ*, 581, 509

- Splaver, E. M., Nice, D. J., Stairs, I. H., Lommen, A. N., & Backer, D. C. 2005, *ApJ*, in press, astro-ph/0410488
- Stairs, I. H. 2003, *Living Reviews in Relativity*, 6, 5
- Stairs, I. H., Splaver, E. M., Thorsett, S. E., Nice, D. J., & Taylor, J. H. 2000, *MNRAS*, 314, 459
- Stairs, I. H., Thorsett, S. E., Taylor, J. H., & Wolszczan, A. 2002, *ApJ*, 581, 501
- Standish, E. M. 1998, *JPL Planetary and Lunar Ephemerides, DE405/LE405*, Memo IOM 312.F-98-048 (Pasadena: JPL), <http://ssd.jpl.nasa.gov/iau-comm4/de405iom/de405iom.pdf>
- Taylor, J. H. & Weisberg, J. M. 1989, *ApJ*, 345, 434
- Thorsett, S. E. & Chakrabarty, D. 1999, *ApJ*, 512, 288
- van Kerkwijk, M., Bassa, C. G., Jacoby, B. A., & Jonker, P. G. 2005, in *Binary Radio Pulsars*, ed. F. A. Rasio & I. H. Stairs (San Francisco: Astronomical Society of the Pacific), in press
- van Straten, W., Bailes, M., Britton, M., Kulkarni, S. R., Anderson, S. B., Manchester, R. N., & Sarkissian, J. 2001, *Nature*, 412, 158
- Weisberg, J. M. & Taylor, J. H. 2003, in *Radio Pulsars*, ed. M. Bailes, D. J. Nice, & S. Thorsett (San Francisco: Astronomical Society of the Pacific), 93
- Will, C. M. & Zaglauer, H. W. 1989, *ApJ*, 346, 366
- Williams, J. G., Turyshev, S. G., & Boggs, D. H. 2004, *Phys. Rev. Lett.*, 93, 261101